Scanning Microscopy

Volume 1 | Number 1 Article 24

10-17-1986

Structure-Function Relationships in Radiation-Induced Cell and Tissue Lesions: Special References to the Contributions of Scanning Electron Microscopy and Hematopoietic Tissue Responses

T. M. Seed
Radiation Hematology Group

Scanning Microscopy, Vol. 1, No. 1, 1987 (Pages 255-272)
Scanning Microscopy International, Chicago (AMF O'Hare), IL 60666 USA

STRUCTURE-FUNCTION RELATIONSHIPS IN RADIATION-INDUCED CELL AND TISSUE LESIONS: SPECIAL REFERENCES TO THE CONTRIBUTIONS OF SCANNING ELECTRON MICROSCOPY AND HEMATOPOIETIC TISSUE RESPONSES

T. M. Seed*

Radiation Hematology Group, Division of Biological and Medical Research
Argonne National Laboratory, Argonne, Illinois 60439-4833 USA

(Received for publication June 25, 1986, and in revised form October 17, 1986)

Abstract

Contributions of scanning electron microscopy to the field of radiation biology are briefly reviewed and presented in terms of an overall goal to identify and characterize the structural features of radiation-induced lesions in vital cell and tissue targets. In the context of "lesion" production, the major radiation-elicited response sequences, the types and nature of measured end points, and governing temporal and radiobiological parameters are discussed and illustrated by using results derived from both *in vitro* cell systems and *in vivo* studies that measured tissue responses from various organ systems (respiratory, digestive, circulatory, and central nervous systems). Work in our laboratory on the nature of early and late hematopathologic tissue responses (aplastic anemia and myeloid leukemia) induced by protracted radiation exposure and the "bridging effect" of repair processes relative to the expression of these pathologies is highlighted.

KEY WORDS: Ionizing radiation, cell and tissue pathology, scanning and transmission electron microscopy, hematopathologies, aplastic anemia, myeloid leukemia.

*Address for correspondence:
Radiation Hematology Group, Division of Biological and Medical Research, Argonne National Laboratory, Argonne, Illinois 60439-4833 USA
Phone No. (312) 972-3865

Introduction

The purpose of this paper is twofold: first, to review the contributions of scanning electron microscopy (SEM) to the field of radiation biology, specifically in terms of the identification and characterization of vital target lesions in cells and tissues following ionizing radiation exposures, and second, to look into the future and suggest possible areas of investigation where SEM might significantly advance current knowledge in the field of radiation biology.

Clearly, SEM has contributed to our understanding of the nature of responses elicited by ionizing radiation exposures. A series of examples is given to highlight this point. It is also clear, however, that SEM has not been used to its fullest potential. The intense focus in recent years by radiation biologists on the elemental molecular and cellular processes has overshadowed morphologic and ultrastructural studies. In part, this overshadowing is unfortunate. For it is the latter techniques that serve to collate, visually, the physical aggregate of the damage registered and repair processes elicited within sensitive cell and tissue targets. However, to come to a full understanding of the nature of induced lesions, such structure-imaging techniques as SEM must be applied to ultimately tie underlying molecular/biochemical events to specific physical changes in targeted cellular components.

Radiological Parameters, Events, and End Points

The essence of an ultrastructural approach in analyzing the nature of radiation-induced damage and repair in targeted cells and tissues lies in the inferences drawn from static images of macromolecular lesion elements and the role these elements play in the induction, progression, or regression (repair) of the lesion itself.

The problem of evaluating radiation-induced damage and repair processes--either by functional or structural parameters--is exceedingly complex because of the number and scope of the parameters: (i) radiation parameters (radiation quality, dose, dose-rate, dose-delivery regimens); (ii) time (radiation and recovery times);

(iii) biological parameters (nature and level of critical targets, i.e., types, number, and relative radiosensitivity and repair capacity) (54). Further, the sheer complexity of biological organization (i.e., from the molecular level to the intact pro- or eucaryotic organism) lends itself to highly variable and exceedingly complex response patterns when coupled to such radiological variables (3,6).

Several of the major biological response routes are illustrated in Fig. 1. Initially, photons or subatomic particles interact with cellular matter resulting in ionizations and, in turn, molecular bond breakage. For every 1 Gy of low linear energy transfer (LET) radiation a cell absorbs, there are an estimated 1000 bond-breaking events in DNA, 3000-3500 in RNA, 20,000 in protein, and 100,000 in cellular water (17). Such marked differences in bond breakage per unit of radiation dose absorbed in the various types of cellular components clearly suggests their relative importance, in terms of subsequent elicited cell response. For the damage to be registered, bond breakage has to occur within vital "targets." Three major subcellular targets have been considered vital: (i) plasma or organellar membranes (Alper's type "O" damage) (2,36,75), (ii) cytoplasmic constituents (e.g., ribosomes, cytoskeleton networks, etc.), and (iii) nuclear components (Alper's type "N" damage) (2). Often, the actual biological mechanism (of reproductive cell death) appears to involve both membranes and nuclei--the so-called cooperative target of the DNA-nuclear membrane anchorage site where replication is initiated (3,17-19,36,37,67,78). Primary events lend themselves, through cascading secondary changes, to damage at higher orders of cell and tissue organization. Damage to vital "targets" results in three broad categories of responses: (i) early effects, (ii) late effects, and (iii) secondary effects (Fig. 1). These response categories are interrelated, both temporally and causally. Secondary effects are indirect and probably the least appreciated and understood of the three response types as to their importance in the final outcome of radiation exposure. For example, radiation damage is expressed in long-term hematopoietic cell cultures in terms of a reduced capacity of the stromal cell microenvironment to maintain both the proliferative and self-renewal functions of free hematopoietic cells of various lineages (14,72). In this case, a radiation-elicited response within one cell type, i.e., stromal cells, is manifested in terms of "feeding" capacity, which in turn effects the viability of a second cell population, and ultimately the tissue system (hematopoietic tissue) at large.

Responses occurring "early" in time are reflected in the primary and secondary biochemical, physiological, and metabolic alterations of the targeted cell and its composite tissue (Fig. 1). The nature and magnitude of such early responses are modified not only by the previously mentioned radiological variables (e.g., dose, dose-rate), but also by time, as it affects the processes of damage accumulation and repair. Generally, we think of a considerable lag time between irradiation and the expression of damage. However, this might not always be true. For example, damage resulting from high LET heavy particles might be instantaneous, due to the penetration of tissue by the extremely large mass ionizing particles (45).

Late effects are causally linked to early responses via repair/recovery-type processes (Fig. 1). Late pathological responses arise as a consequence of residual damage resulting from either incompletely repaired or misrepaired (error-prone) subcellular or cellular processes. Mutation, transformation, reduced proliferative potential, enhanced rates of senescence, etc., are some of the more prominent examples of late effects at the cellular level. Affected cells often display an array of structural modifications characteristic of the given late effect. For example, in the work of Borek and Fenoglio (7), an abnormal cell-cycle-independent expression by CHO cells of high-density surface microvilli occurred as a consequence of neoplastic transformation following x-irradiation. At the organ/organismal level, related responses such as the development of cancer and various types of degenerative diseases are prominent late effects of ionizing radiation exposure. The radiobiological parameters that affect such "early" to "late" transitions will be illustrated more fully by our work in developmental sequences of leukemogenesis under chronic ionizing radiation exposure.

Models of Tissue Response

A variety of cell and tissue-response models have been used to evaluate the physiological, biochemical, and morphological nature of radiation-induced damage and repair. A sampling of those studies that have used surface imaging ultrastructural methods--primarily SEM--are listed in Table 1. I will simply highlight a few of the more important observations, then will describe some of the current work in my lab, which should illustrate the biological consequences of these various radiological parameters.

Mammalian cells, in vitro

Despite the myriad of induced topographic lesions, common response patterns are evident (Table 1). For example, the extensive surface blebbing and ruffling seen following relatively high dose exposures (>10 Gy) is probably a time or dose-dependent manifestation of early occurring, unrepaired surface lesions, such as the ones seen in primary human embryo fibroblasts minutes following low-dose exposures (24-27,42, 66,77). In terms of "late effects" of radiation exposure, these induced surface responses, elicited early following exposure, seemingly become a constitutive part of the phenotype of the transformed, neoplastic cell (7).

Gastrointestinal system

Because of its cell renewing-amplifying nature, the gastrointestinal (GI) tract is one of the more radiosensitive organ systems and, as a consequence, is often dose-limiting under various radiotherapeutic protocols. As such, extensive sets of kinetic and radiobiological

Table 1. Radiation Parameters, and Measured End Points in Cell/Tissue Response to Ionizing Radiation.

SPECIMENS	RADIATION PARAMETERS: TYPE (X-RAY, GAMMA, NEUTRON, PROTONS, ALPHA, BETA, H-IONS)	DOSES (Gy) (>1, 1-10, 11-20, >20)	REGIMEN (SINGLE, ACUTE; CONTINUOUS; FRACTIONATED; TOTAL; PARTIAL)	ANALYSIS: TYPE (LM, TEM, SEM, PHYSIOL, BIOCHEM)	SITE (IN VITRO, IN VIVO)	LEVEL (ORGANISM, TISSUE, CELL, SUBCELL)	MAJOR END POINTS	REFERENCES
MAMMALIAN CELL LINES								
T-LYMPHOBLAST (MOLT-4) FIBROBLASTS (V79); HAMSTER	•	• • •	•	• • • •	•	• •	SURFACE/NUCLEAR TOPOGRAPHY; CHROMATIN STRUCTURE	(69)
LYMPHOBLASTOID CELLS; RAT (L5178Y)	• •	• •	•	• • •	•	• •	SURFACE TOPOGRAPHY; LECTIN RECEPTORS; ELECTROPHORETIC MOBILITY; MEMBRANE FLUIDITY	(77)
FIBROCYTOID/EPITHELOID; MOUSE, (10T1/2 CELLS)	•	•	•	• •	•	• •	CELL/NUCLEAR SHAPE; TRANSFORMATION	(38)
10T1/2 SPHEROIDS	•	• •	•	• • • • •	•	• • •	MELANIN PRODUCTION; RADIOSENSITIVITY; CELL GROWTH; CLONING	(70)
EMBRYO CELLS; HAMSTER	•	•	•	• •	•	•	SURFACE TOPOGRAPHY; CELL GROWTH, TC MEDIA/AGAR	(7)
EMBRYO FIBROBLASTS; HUMAN	•	• •	•	•	•	•	SURFACE TOPOGRAPHY; CELL-SUBSTRATE ATTACHMENTS	(66)
FIBROBLASTS (HeLa; CHO)	•	• • •	•	•	•	• •	NUCLEAR PORES; SIZE/DENSITY	(68)
GLIAL CELLS; HUMAN	•	•	•	• •	•	•	SURFACE TOPOGRAPHY; PLASMALEMMAL TURNOVER	(26)
GLIAL CELLS; HUMAN	•	• • •	•	• • •	•	• •	SURFACE TOPOGRAPHY; LYSOSOME STRUCTURE	(24)
LYMPHOHEMATOPOIETIC TISSUE								
HEMATOPOIETIC CULTURE; MOUSE	•	• • •	•	• • • •	•	• •	CELL GROWTH; CYTOCHEMISTRY	(72)
THYMOCYTES; RAT	•	•	•	• •	•	• •	MICROVILLI; CELL VIABILITY	(76)
THYMOCYTES; RAT	•	•	• •	•	•	• •	MICROVILLI; CELL SIZE; CELL FRAGMENTATION	(49)
BONE MARROW; DOG	•	• • •	• •	• • • •	•	• • •	MARROW PARENCHYMA STRUCTURE; APLASTIC ANEMIA; LEUKEMIA	(55)
BONE MARROW; DOG	•	• • •	• •	• • • •	•	• • •	ENDOSTEAL STRUCTURE; FIBROSIS	(56)
BONE MARROW; DOG	•	• • •	• •	• • • •	•	• • •	MEGAKARYOCYTE STRUCTURE; LEUKEMIA	(73)
ERYTHROCYTES; HUMAN	•	•	•	•	•	•	SHAPE TRANSFORMATION	(47)
GASTROINTESTINAL								
SMALL INTESTINE; MOUSE	• •	•	• •	• • •	•	• •	VILLUS, CRYPT SHAPE	(11)
SMALL INTESTINE; MOUSE	• •	• •	• •	• •	•	• •	STROMAL ELEMENTS	(10)
SMALL INTESTINE; MOUSE	•	•	• •	• • •	•	• •	VILLUS STRUCTURE; GIANT CELL FORMATION	(13)
SMALL INTESTINE; MOUSE	• •	•	•	•	•	• •	VILLUS STRUCTURE; GIANT CELL FORMATION	(33)
SMALL INTESTINE; RAT	•	• • •	• • •	•	•	• • •	VILLUS, CRYPT STRUCTURE; GOBLET CELLS; PEYER'S PATCHES	(20)
SMALL INTESTINE; RAT	•	•	•	• •	•	• •	VILLUS STRUCTURE	(4)
SMALL INTESTINE; MOUSE	• • •	• • •	• • •	•	•	• •	VILLUS STRUCTURE; GOBLET CELLS	(8)
SMALL INTESTINE; RAT	•	•	•	•	•	• • •	EPITHELIAL TIGHT FUNCTIONS	(53)
SMALL INTESTINE; MOUSE	•	•	•	• •	•	• • •	MUCOSAL LAYER; BACTERIAL COLONIZATION	(74)
SMALL INTESTINE; MOUSE	• • •	• • •	• • •	•	•	• •	VILLUS STRUCTURE	(12)
SMALL INTESTINE; MOUSE	• •	•	• • •	• • •	•	• •	VILLUS STRUCTURE; CRYPT NUMBER	(9)
STOMACH, SMALL INTESTINE; MOUSE	•	• •	• •	•	•	• •	CAPILLARY, ARTERIAL, VENOUS VASCULATURE	(16)
RESPIRATORY TRACT								
LUNG; MICE	•	• •	•	• • • •	•	• • • •	ALVEOLUS STRUCTURE; PNEUMONITIS; FIBROSIS	(51)
LUNG; MICE	•	• • •	•	• • •	•	• • •	ALVEOLUS STRUCTURE; PNEUMONITIS; FIBROSIS	(41)
TRACHEA; RABBIT	•	•	• •	• • • •	•	• • •	CILIARY STRUCTURE; BEAT-FREQUENCY; GOBLET; EPITHELIAL CELL STRUCTURE	(1)
BRONCHIAL LAVAGE; RAT	•	• •	•	• • •	•	• •	SURFACE RUFFLING/PITS; CELL VIABILITY; PHAGOCYTIC FUNCTION	(42)
EYE								
RETINA; RAT	•	•	•	•	•	• •	RETINAL ROD STRUCTURE	(45)
RETINA; RABBIT	•	•	•	•	•	• •	RETINAL ROD/CONE STRUCTURE	(48)
URINARY SYSTEM								
KIDNEY; RAT	•	•	•	•	•	• •	MICROVASCULATURE	(46)
CNS								
BRAIN; MAN	•	• •	• •	• •	•	• •	CILIA STRUCTURE; SURVIVAL	(23)
HYPPOCAMPI; RETINI; MICE	•	•	•	• • •	•	• •	SYNOPTIC DENSITY; MOTOR FUNCTION	(52)

response data have been collected on this tissue system. Topographic analyses, via SEM and related techniques, of villus and cryptal structures (4,8-13,16,20,28,29,53,74), supporting capillary network, and mucosal layer have provided new insights into functional aspects of the damage and repair responses of this tissue to ionizing radiation (Table 1). Some of these responses have proven to be more sensitive indications of the extent of radiation-induced damage to the "functional compartments" of the system than the standard microcolony assay for intestinal crypts in the "proliferative zones" (9).

Respiratory tract

The lung is a primary dose-limiting tissue in thoracic radiotherapeutic protocols probably because of the development of two prominent, late-arising pathological events, i.e., pneumonitis and fibrosis that often follow high, local tissue doses (>12 Gy). In combination with transmission electron microscopy (TEM), SEM has aided in the identification of the principal cells involved in the development of these two major pulmonary pathologies: pneumonitis, due to response of principally type II pneumocytes and their induced surfactant secretions and pulmonary macrophages that serve to turn over surfactant, and fibrosis, due principally to an interstitial macrophage-dependent fibrogenic response by fibroblasts (41,51).

Eye tissue

Unique SEM images of retinal tissue damage following both low- and high-LET irradiations have been obtained (45,48). Both qualities of radiation adversely affect rods and cones to a greater extent than other visual elements: low-LET x-irradiation (70 Gy) induces rather widespread swollen, bent, and irregular photoreceptors (48); in contrast, high-LET iron ions (~2 Gy) produce highly localized tracks through the retinal tissue. In the latter case, photoreceptors appear normal in the nontracked areas but completely blown away where the ions had apparently penetrated (45). Interestingly, the density of the ion tracks is about twofold less than the density predicted from ion fluence measurements. Further, the "bore-size" of the densely ionizing iron particle appears to be about 10-20 μm, which is roughly about a magnitude less than predicted by certain particle track models (40).

Vascular system

Through the use of resin casting, vascular networks of several organs (e.g., spleen, kidney, liver, stomach, intestine) have been studied under various radiation protocols (16,46). Differential responses have been observed, depending on the postirradiation time, initial dose of irradiation, and species of network being evaluated. According to the work of Egawa and Ishioka (16), the vasculature of the small intestine is most radiosensitive (in the dose range of 5-30 Gy, in times ranging from 1-30 days postirradiation), whereas the kidney vasculature appears to be the least sensitive.

Hematopoietic Tissue

Work in my own lab will serve to illustrate early and late hematopoietic tissue responses to ionizing irradiation--in this case delivered chronically to the exposed individual in low daily doses.

Leukemia as a biological end point figures prominently into the "risk" assessment process because of its natural rarity, relatively high rates of induction, and short latency following exposure. Most of what is known about its nature and incidence comes from acute, high dose or dose-rate-type exposures, and not from protracted low dose or dose-rate-type exposures. There is a paucity of information regarding the leukemogenicity of chronically delivered low daily doses of ionizing radiation. The report of the Committee on the Biological Effects of Ionizing Radiations (BEIR) (15) states, "Until we know the radiobiological basis for leukemia induction (and progression) we cannot be confident regarding choice of model or parameter values for use in risk calculations in the low-dose region." In addressing this issue, we have been attempting to map out, using a canine model, critical temporal and radiobiological determinants of the chronic radiation-induced leukemogenic response. The model uses young beagles (400 days old) exposed to whole-body gamma irradiation delivered chronically in low daily doses (1.9-7.5 cGy/22 h day) for either fraction- or duration-of-life (Fig. 2). Our approach to the work has involved the serial assessment of the hematopoietic system of each individual with respect to time of exposure, total accumulative radiation dose, and preclinical phase.

Differential Hematopoietic Responses of Subgroups. On the basis of survival and pathological predisposition, two distinct responding subgroups under chronic gamma irradiation have been identified: i.e., radiosensitive (S^-) short-term surviving, aplastic anemia-prone (AA-prone) dogs versus radioresistant (R^+) long-surviving, myeloid leukemia-prone (ML-prone) subgroups (Fig. 3). These subgroups are functionally defined not only at the organismal level, but also at the levels of the hematopoietic organ and of the hematopoietic progenitor target cells. The major distinguishing trait of these subgroups is in their "hematopoietic recovery or repair potentials" exhibited under chronic radiation regimens. To illustrate the difference in repair potential of the hematopoietic system between the subgroups, the sequential change in absolute marrow cellularity and the estimated granulocyte reserves are shown in Figs. 4 and 5, respectively. In the case of the AA-prone individual, the marrow cellularity and reserves are progressively depleted over the time course of exposure. In contrast, the ML-prone individual initially responds with a progressive decline in cellularity and reserves, but at 200-300 days of exposure the rate of marrow cell loss slows down, then stabilizes, and is replaced by partial recovery. Simply put, these changes, along with a number of other parameters assayed, are manifestations of a repair-deficient hematopoietic system in the radiosensitive, AA-prone subgroup, and a repair-proficient hematopoietic system in the radioresistant, ML-prone subgroup. In terms of the

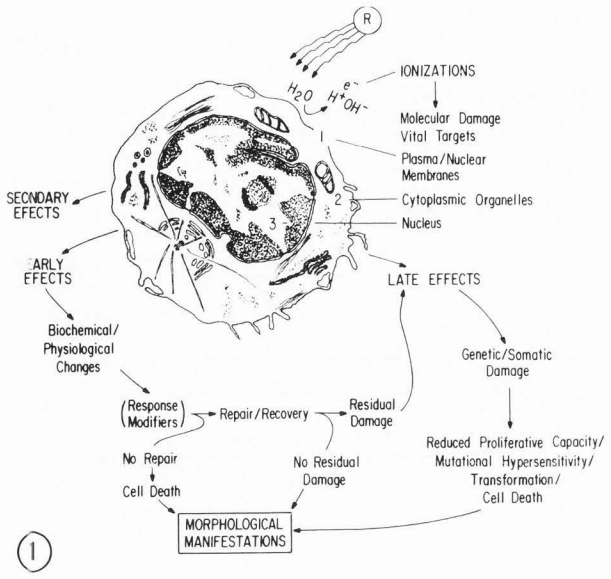

Fig. 1. Schematic of potential response sequences of irradiated mammalian cells.

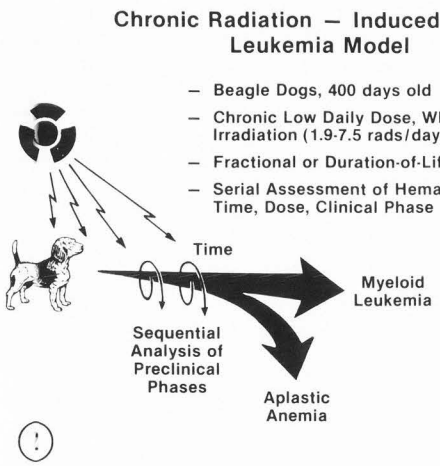

Fig. 2. Primary features of the chronic radiation leukemogenesis model.

3

RESPONDING SUBGROUPS

Sensitive S^-	Resistant R^+
Radiosensitive (Animal → Organ → Target Cell)	Radioresistant (Animal → Organ → Target Cell)
Recovery/Repair Deficient	Recovery/Repair Proficient
Aplastic Anemia-Prone	Myeloid Leukemia-Prone

Fig. 3. Characteristics of animal subgroups responding to chronic radiation stress.

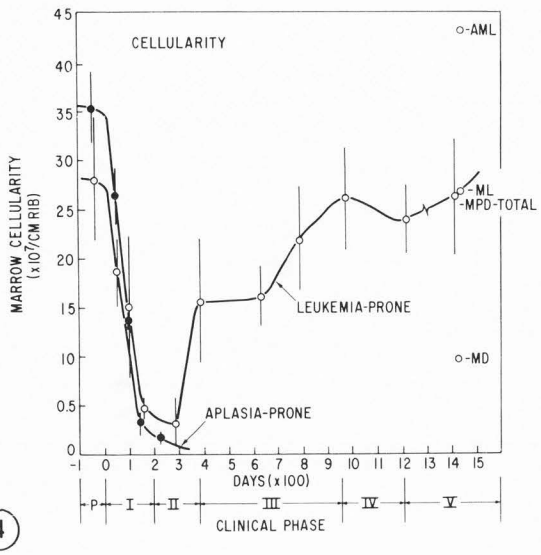

Fig. 4. Sequential change in bone marrow bone cellularity with time of chronic irradiation and preclinical phases of developing aplastic anemia (aplasia-prone) and myeloid leukemia (leukemia-prone) (60).

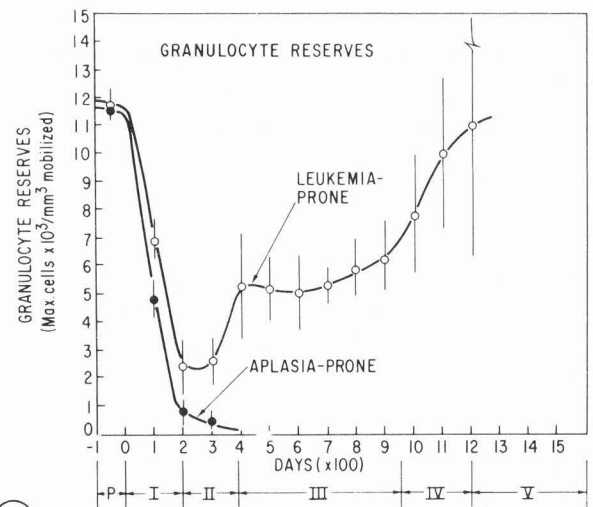

Fig. 5. Change in bone marrow granulocyte reserves of irradiated dogs progressing to either aplastic anemia or to myeloid leukemia (60).

leukemogenesis, induction of hematopoietic repair within the proficient animal serves to "bridge" early and late preclinical periods, thus fostering the development of myeloid leukemia.

Morphological Analysis. SEM has contributed significantly to the monitoring of the marrow response within the two subgroups (Figs. 6-19). Clearly shown is the overall extent to which

marrow is restructured during the development of aplasia (Figs. 10-13). With pathological progression, lipid-laden adipocytes increase in size, and perhaps in number, at the expense of a declining number of free hematopoietic cells. In contrast, the marrow of the ML-prone individual (compared to marrow of the AA-prone individual) exhibits, at the nadir of the suppressive response, a lower fat/hematopoietic cell ratio, increased stromal matrix, and subsequently, in the postrecovery phase, a hemoproliferative response that further reduces the fat/cell ratio (Figs. 14-19) (64).

During these sequential morphological analyses, it became obvious that the endosteum--the functional cellular interface between bone and hematopoietic parenchyma--was being altered in a differential fashion in the select subgroups of animals. The endosteum is a vital part of the hematopoietic microenvironment (HIM), providing a source of hematopoietic stem cells and stromal cell progenitors, alike (22, 50), in addition to carrying out its chief responsibility, namely, bone remodeling. In the context of the previously noted repair potentials of the two subgroups, it is clear that to initiate the repair sequence there must be first, activation of quiescent endosteal bone surfaces to formative and resorptive areas; second, a proliferation-dependent restructuring of the microvasculature-stromal network; and third, reseeding of newly formed stromal niches with hematopoietic progenitors. In this regard, SEM has provided us with a very useful way to survey large expanses of endosteal surface, and, thus, monitor with time of exposure and pathological progression differential responses of the subgroups (Figs. 7, 8, 11, 13, 17, 19). Results of such analyses have shown that (a) in the AA-prone animals, the extent of endosteal area devoted to formative and resorptive activity is reduced with corresponding increases in quiescent areas and (b) in the ML-prone animals, the shift in endosteal activity is in the opposite direction, i.e., from quiescent to active. These differential endosteal responses clearly influence hematopoietic regenerative capacity and, in turn, the development of the major classes of hemoproliferative disorders under chronic gamma irradiation (55,56).

Analyses of Hematopoietic Progenitors. The origin of the degenerative/ regenerative marrow responses, as noted above, is at the stem cell and early progenitor compartments. These cells assume highly pivotal roles in the pathogenesis of these major hematopathologies developed under chronic gamma irradiation. Because of the prominence of myeloid leukemia, we have focused our analyses on the early progenitor compartments committed to granulocyte, monocyte differentiation (GM-progenitors or GM-CFUa). In terms of leukemia induction, it is at this level that the transformed phenotype is expressed. These cell types are highly regulated, in part through a series of positive and negative feedback loops involving both mature progeny and stromal elements (39,43). Presumably, because of the degree to which these critical "targets" are regulated, they are highly susceptible to interruptions in regulation under chronic irradiation. In the context of the two major hematopathologies that we are dealing with here, leukemia is considered to be the result of exaggerated "self-renewal" coupled with blocked differentiative processes (44), whereas aplastic anemia is the result of restricted self-renewal coupled with reduced pluripotent stem cell input and unabated differentiative flow.

In vitro cloning of GM-committed hematopoietic progenitors, with our standard double-layer agar system, provides for both quantitation of progenitors from given marrow sources and determination of qualitative features associated with their proliferative and differentiative properties (57,61). Cloned normal and leukemic progenitors are shown in Figs. 20-27.

The sequential change in marrow concentration of these vital GM-progenitors with time of irradiation in the two subgroups is shown in Fig. 28. These response patterns closely parallel the previously noted phase-related cellular changes in total marrow cellularity and mature cell reserves: in the AA-prone subgroup, the number of GM-CFUa progressively declines, reaching ~1% of preirradiation levels by 200-330 days of exposure; in the ML-prone subgroup, there is an initial suppression (preclinical phase 1) over the first 150-200 days, followed by partial recovery (preclinical phase 2) between 200-300 days, and subsequent accommodative fluctuations in number thereafter (preclinical phase 3). Entry into the late preclinical phases (preclinical phase 4) is signaled by the decline in numbers of "normal" colony-forming progenitors, with progressively increased numbers of cell clusters (61,62).

As I previously mentioned, these committed stem cells come under the regulatory influence of HIM, i.e., both stromal cell and humoral factors, alike. Serum titers of colony-stimulating factors (CSA), i.e., the suspected granulo- and monopoietins for GM-committed marrow progenitors, rise reciprocally with falling marrow levels of GM-committed stem cells during early phases of irradiation (Fig. 29): CSA titers tend to be higher in sera from AA-prone dogs than in the ML-prone dogs during its initial prerecovery phase of evolving ML. Conversely, CSA titers fall as the rate of suppression of GM-committed progenitors slows, stabilizes, and subsequently exhibits renewed proliferative activity (Fig. 29).

Although the stromal network of the marrow is generally assumed to be relatively radioresistant (in terms of the low daily dose rates used in these studies), elements of the supporting network, namely reticular cell progenitors (CFUf), derived from marrow samples of both major subgroups, are initially suppressed during the initial irradiation period, and either fail to recover, in the case of the aplasia-prone dogs, or fully recover and stabilize in number in the case of the ML-prone animals.

Mechanisms of Hematopoietic Recovery. Two points are important in evaluating the quantitative changes in number of hematopoietic progenitors with time of irradiation (as shown in Fig. 28): First, recovery occurs in the face of

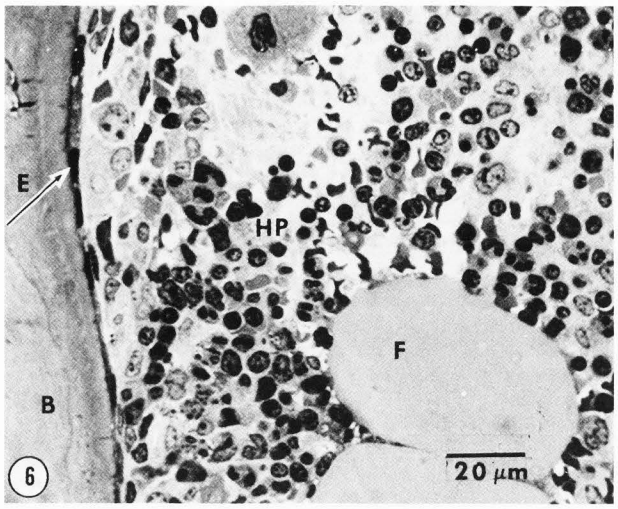

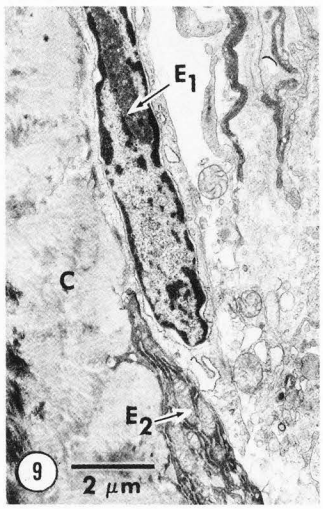

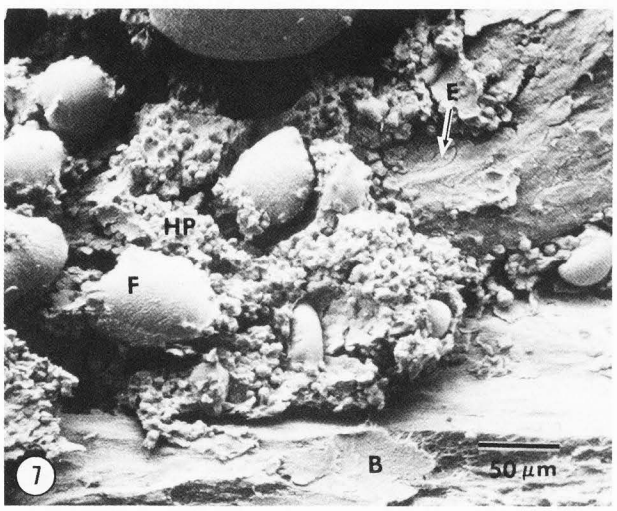

Figs. 6-9. Characteristic features of 'normal' bone marrow from control, unirradiated young adult dogs (56). Abbreviations used in these figures are common to all subsequent figures. Fig. 6. Light micrograph (LM) showing hematopoietic parenchyma (HP) filled with mature and immature hematopoietic elements (erythroid, granuloid, and megakaryocytic elements) and interspersed with lipid-laden adipocytes (F). The thin endosteal cell layer (E) forms the interface between marrow and bone (B). Fig. 7. Low-power scanning electron micrograph (SEM) surveys the overall topographical features of the unperturbed hematopoietic elements (HP), the endosteum (E), and bone (B). Fig. 8. SEM illustrates the surface details of the normal endosteal cell layer (E) from the unirradiated animal. Fig. 9. Transmission electron micrograph (TEM) shows the cytological details of the two dominant, thin, endosteal cells (E-1, light cells; E-2, dark cells) as they cover the partially mineralized collagen bed (C).

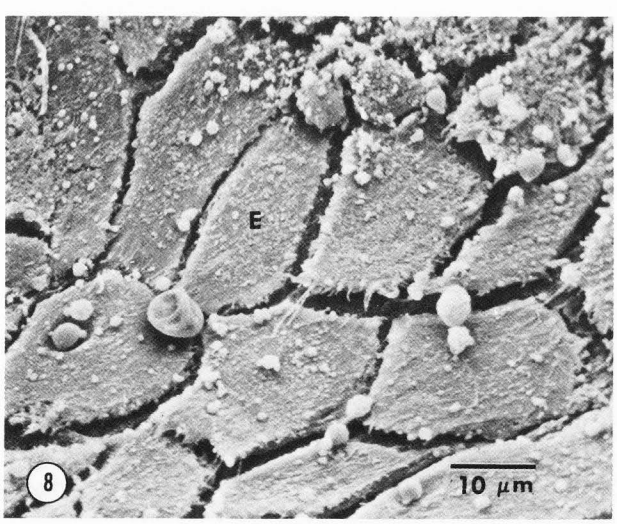

continuous irradiation, implying that the regenerating hematopoietic progenitors have acquired increased radioresistance. Second, continuous irradiation exerts various degrees of "selective pressure" on the responding progenitor population, depending upon the daily rate of exposure. In regard to the latter, we are currently assessing this selective pressure effect on GM-progenitors under various rates of daily exposure (1.9-12.8 cGy/day). Results indicate that the overall suppression of the targeted GM-progenitor population declines as the daily dose rate declines: from 70% at the 7.5 cGy/day dose rate, to 20% at 3.8 cGy/day, and to 9% at 1.9 cGy/day. In a related fashion, the incidence rate of ML in the long-surviving animals falls as the exposure rate declines, i.e., from 44% at 7.5 cGy/day, to 36% at 3.8 cGy/day, and to 10% at the 1.9 cGy/day dose-rate. In the context of ML induction under continuous duration-of-life radiation exposure, the ML

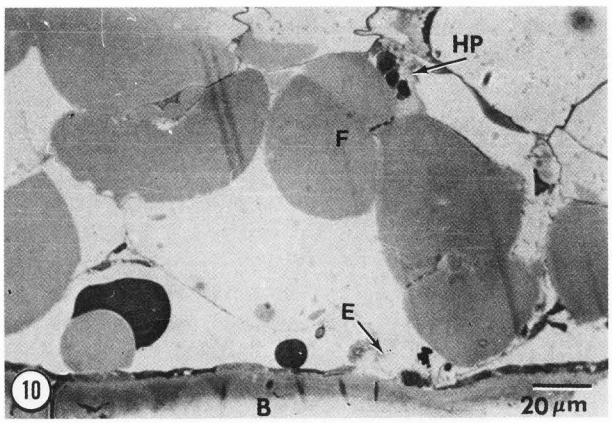

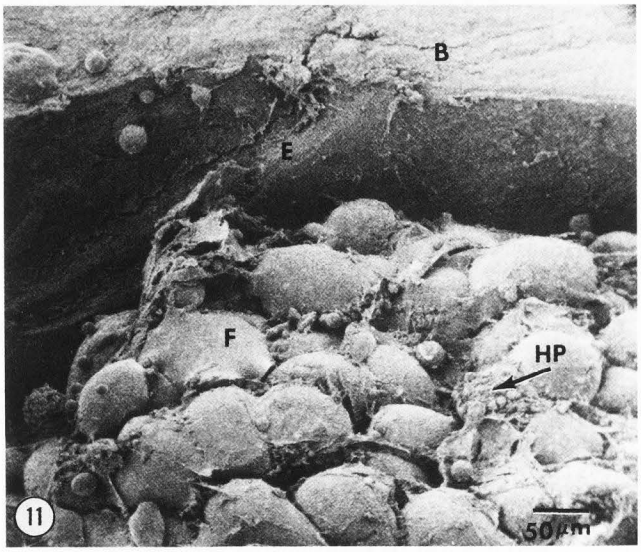

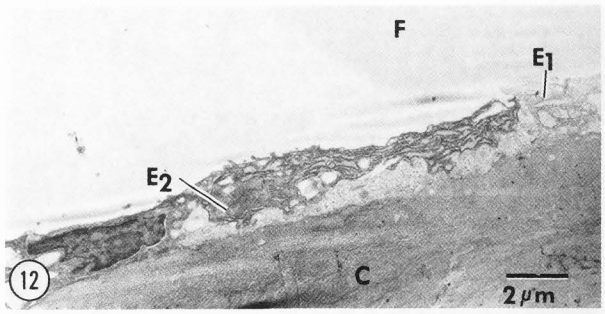

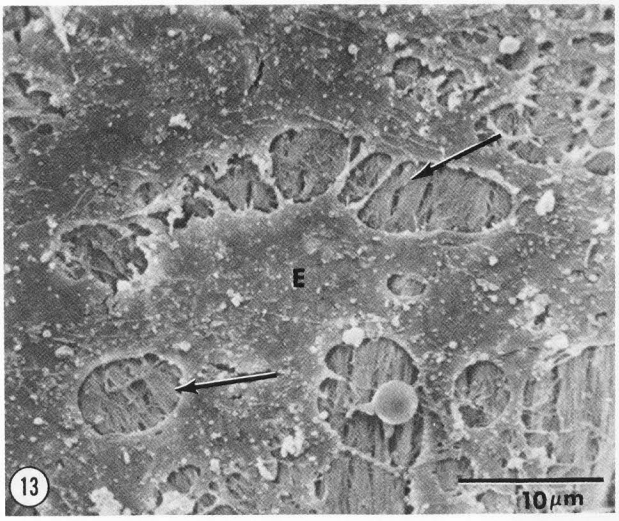

Figs. 10-13. Representative morphological features of bone marrow from the chronically irradiated, radiosensitive [S^-] subgroup during late phases of progressing aplastic anemia. Fig. 10. LM showing marked hematopoietic cell (HP) depletion with corresponding increases in marrow fat (F) (55). A thin, quiescent endosteal cell layer (E) has focal lesions (arrow). Fig. 11. Low-power SEM topographically highlights the dramatic change in marrow architecture: markedly increased marrow fat (F) and loss of hematopoietic elements (HP). Fig. 12. TEM shows the ultrastructural details of the quiescent dark endosteal cells (E_2), and the degenerative features of the light cells (E_1). Fig. 13. Face-on-view by SEM of the quiescent endosteal layer (E) characteristically reveals large intercellular gaps (lesions) (arrows) and the underlying collagen bed.

incidence curve for the long-surviving, repair-proficient, ML-prone animals appears "bell-shaped" with peak ML incidences occurring at the 7.5 cGy/day dose-rate (60). The incidence curve is apparently restricted at the lower dose rates (<7.5 cGy/day) by the selective pressure effect exerted on the potentially transformable, targeted hematopoietic progenitors, while at the higher dose rates (>7.5 cGy/day), the response is restricted by excessive target cell killing.

The product of this selective pressure is the outgrowth of a markedly radioresistant, highly transformable hematopoietic progenitor clonotype. The point made earlier, that the noted renewed proliferative activity by GM-progenitors of the ML-prone dogs following 200-300 days of continuous irradiation, implied that the population had acquired radioresistance. This concept was quickly verified by direct assay, *in vitro*, of the inherent radiosensitivity of these cells (Fig. 30) (61,63). We subsequently mapped out the temporal sequence of the change in target cell radiosensitivity and have clearly demonstrated that the transition (from low to high radioresistance) occurs with entry into the hematopoietic recovery phase.

The latter raises the question as to whether this shift in radiosensitivity is due to simple selection of a preexisting radioresistant subpopulation of progenitors, or due to a mutational event coupled with subsequent selection. Through sequential analyses of the early responses, we have tentatively ruled out "simple selection" as a primary mechanism of acquired radioresistance. In these studies, we could not detect a gradual and progressive outgrowth of radioresistant clonotypes, starting at the time

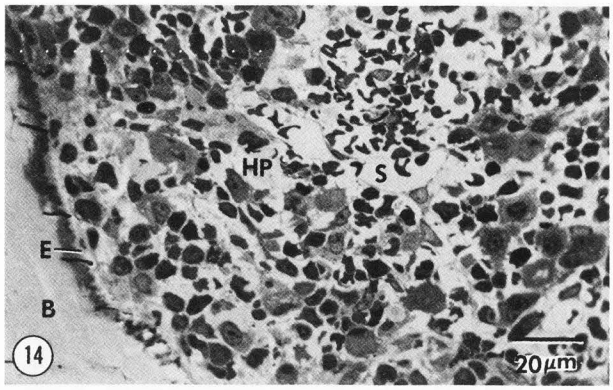

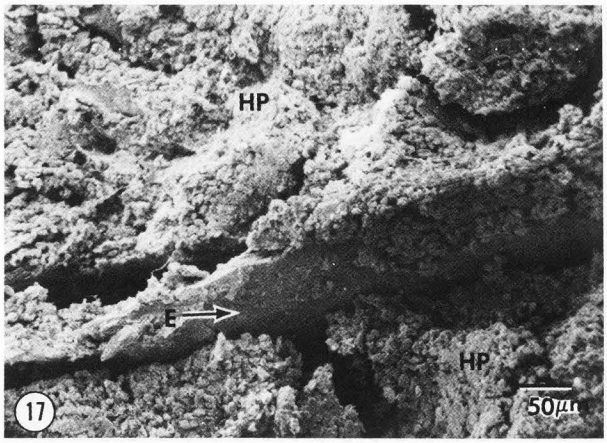

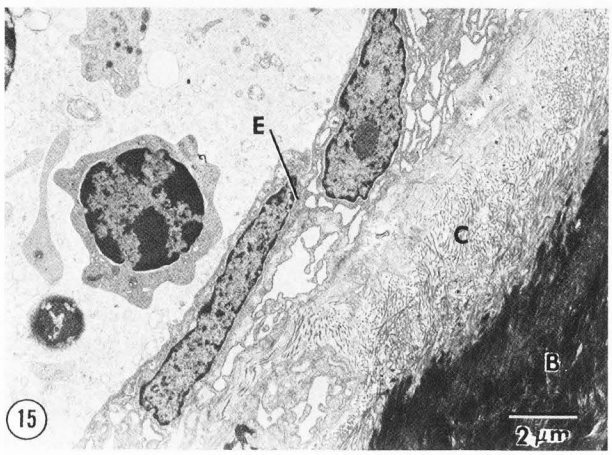

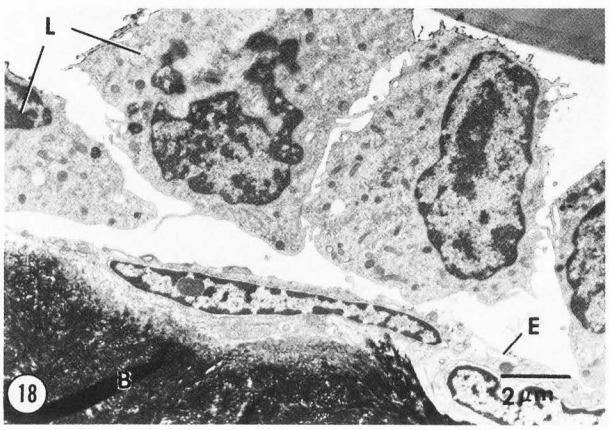

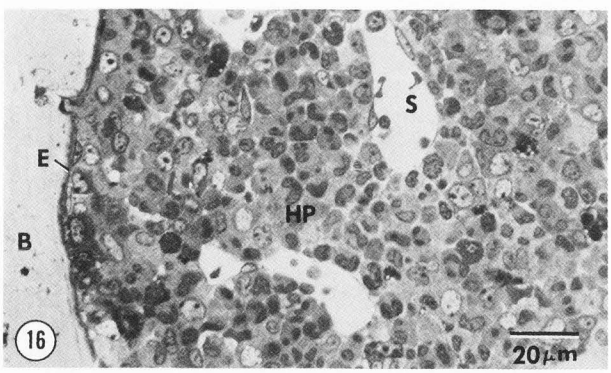

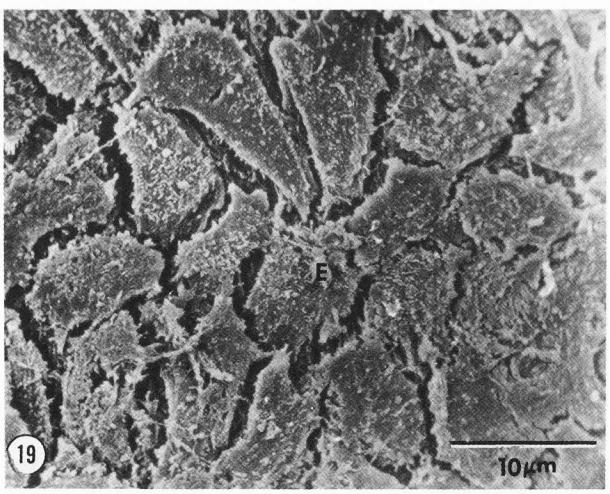

Figs. 14-19. Morphological features of bone marrow from chronically irradiated [R^+] subgroup dogs in early and late phases of progressing myeloid leukemia. Fig. 14. LM showing hypercellular, low-fat marrow with reactive endosteum during an early preleukemic period (55). Fig. 15. TEM showing details of the hypertrophic endosteal layer during early preleukemic phase. Fig. 16. LM of patently leukemic marrow. Fig. 17. Low-power SEM of leukemic marrow showing characteristic hypercellular, low-fat features. The surface of the trabecular ridge (arrow) is fully lined with low-lying light endosteal cells (E) and closely associated leukemic cells. Fig. 18. TEM showing leukemic cells (L) in close association with thin electron light endosteal cells (E). Fig. 19. SEM showing face-on view of the endosteal layer (E) of patently leukemic marrow.

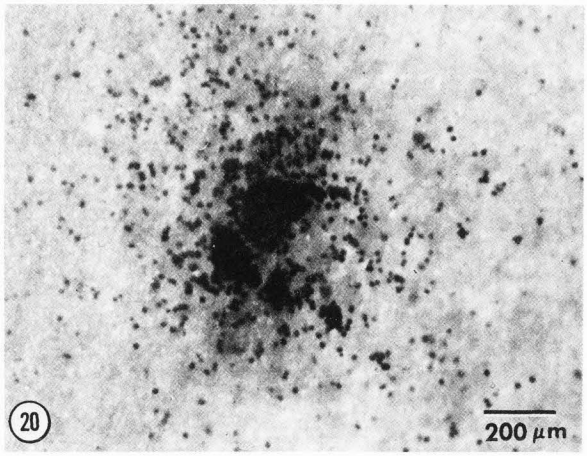

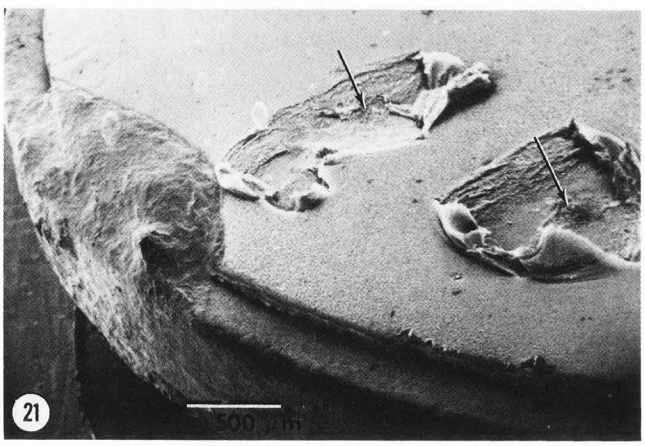

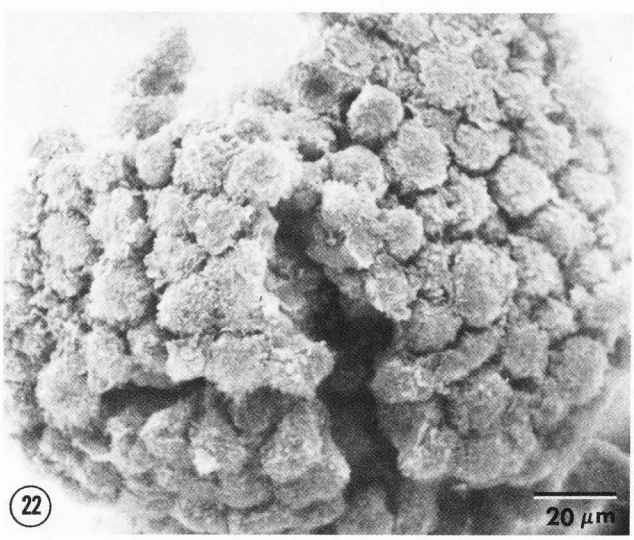

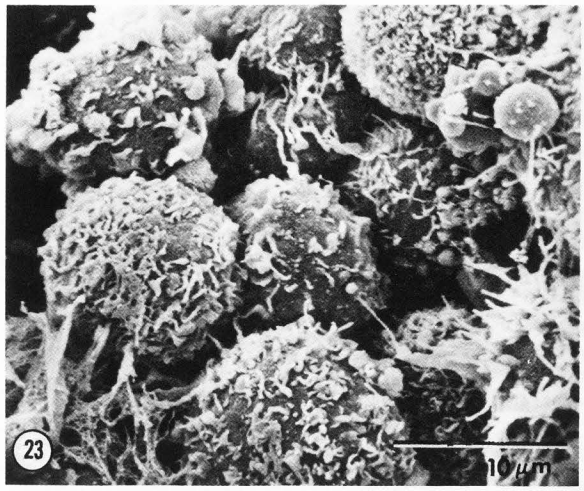

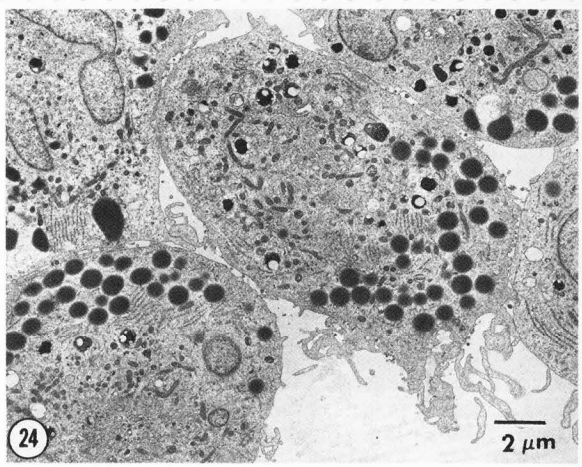

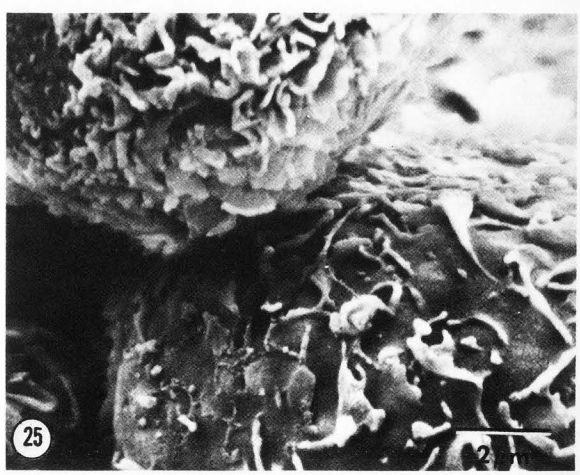

Figs. 20-25. Morphological features of in vitro cloned hematopoietic progenitors from control animals. Fig. 20. Typical GM-CFUa colony derived from marrow progenitors of an unirradiated control dog (57). Fig. 21. Low-power SEM showing a mounted agar slab, prepared for SEM viewing. Two agar-embedded colonies are exposed (arrows) following teasing away the overlying agar (57). Fig. 22. By SEM, a nearly intact hematopoietic colony is shown following excision from the embedding agar. Fig. 23. Surface features of cloned 'normal' cells shown. Fig. 24. TEM of cloned 'normal' hematopoietic progenitors (57). Fig. 25. A high-power SEM revealing surface details of cloned cells (57).

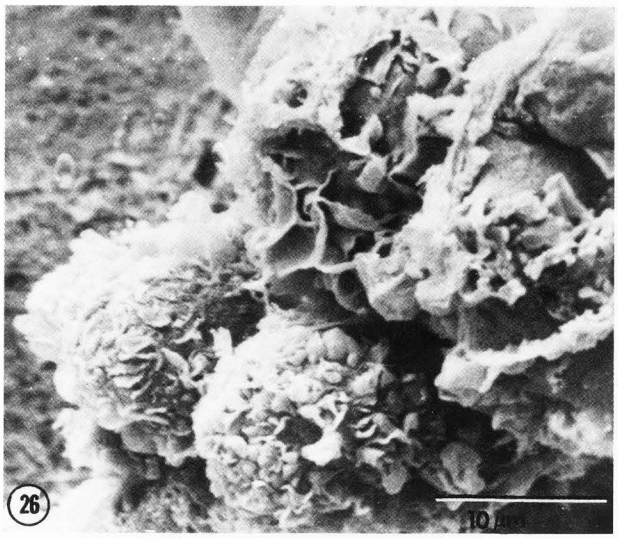

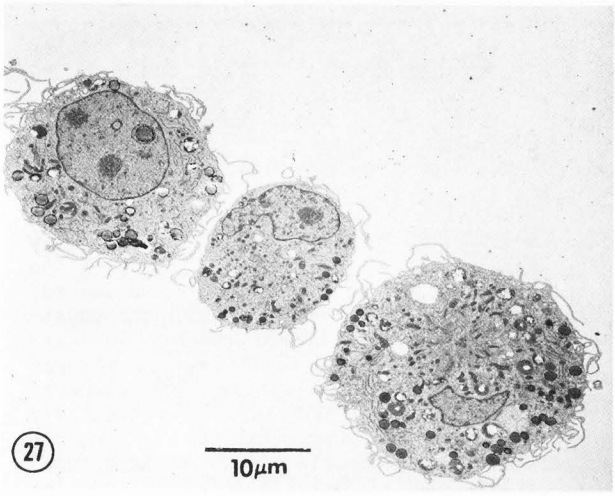

Figs. 26 and 27. In vitro cloned hematopoietic cells from a patently leukemic dog. Fig. 26. SEM reveals the dominant surface feature, i.e., large ruffles, on in vitro cloned leukemic cells. Fig. 27. TEM of in vitro cloned leukemic cells near the edge of colony is shown.

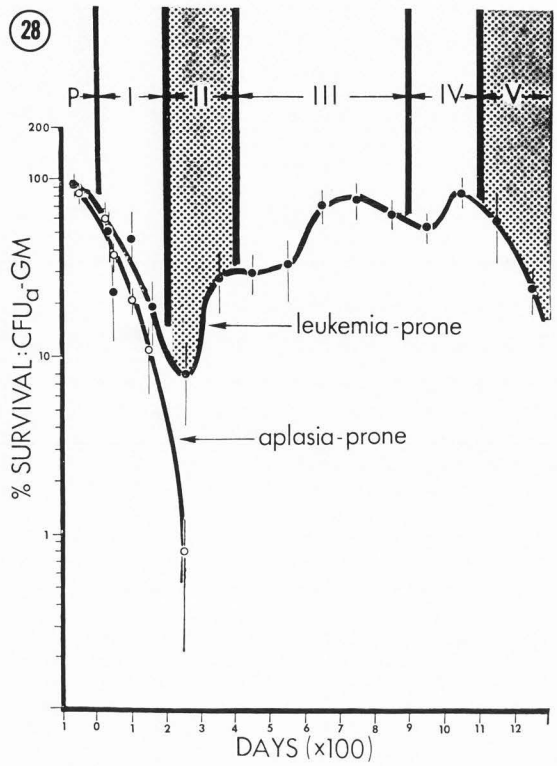

Fig. 28. Change in hematopoietic progenitor cell (GM-CFUa) number in marrow of radiosensitive [S^-] aplasia-prone subgroup versus radioresistant [R^+] leukemic-prone subgroups of dogs with time of exposure and preclinical phase progression.

of exposure, as would be predicted if "simple selection" was operative. In contrast, the GM-progenitors appeared to have increased radiosensitivity (relative to controls or to preirradiation samples) during this initial exposure period. Despite these findings, however, simple selection cannot be entirely ruled out because of the possibility of a "clearing requirement", i.e., clearing of receptive hematopoietic niches within HIM of the initially dominant radiosensitive population prior to reseeding and outgrowth of the radioresistant population.

During a review of the work on radiosensitivity testing of hematopoietic progenitors, it became clear that multiple response patterns were being expressed and that these distinct survival patterns reflected specific clonotypes (60). In the context of pathological progression to aplastic anemia, the normal radiosensitive clonotype (X) remained dominate, despite the small increases in expression of two radioresistant clonotypes (A&C) (Fig. 31). Similarly, in progression to ML during the initial prerecovery phase, the normal radiosensitive clonotype (X) remained dominate, but, in contrast, was rapidly replaced, initially, by the resistant clonotypes A, B, and later by C. This change in frequency suggests that during pathological progression there is clonal succession of distinct radioresistant GM-progenitor populations (Fig. 32).

The work described above has generated a number of questions--questions that we would dearly like to have answered. What is the molecular basis of the acquired radioresistance expressed by committed progenitors of the ML-prone individual? Conversely, why is this resistance not expressed by progenitors of the AA-prone? Clearly, the basis of such radioresistance might be due to a number of factors, working singly or in combination. Some of these factors might include repair processes, selected cell-cycle modifications, or perhaps extracellular microenvironmental effects. Selected studies have been carried out to probe the importance of these factors. For example, such possible microenvironmental effects as the differential

induction by chronic radiation of elevated levels of superoxide dismutase (SOD)--a potent free radical quenching enzyme--in marrow elements of the two subgroups has been explored. In contrast to our expected results, the data indicated that only blood and marrow elements from the AA-prone dogs were significantly different from the control tissues, in that markedly reduced levels were noted. A variety of other microenvironmental effects, e.g., chronic tissue hypoxia, have been considered as well, but the results have been inconclusive.

The influence of cell-cycle modifications has also been evaluated in terms of its potential as a mediator of altered radioresistance. Two approaches have been used: First, we have used ^{3}H-thymidine or cytosinarabinoside suiciding protocols to measure the S-phase fraction of progenitor populations at various times of exposure or pathological phases. Second, we have directly tested the radiosensitivity of S-phase-depleted progenitor preparations. Results of both assays suggest that during the initial, radiotoxic phase of exposure, the S-phase fraction of the GM-progenitor population is enlarged, imparting increased radiosensitivity in both subgroups of animals (AA-prone; ML-prone). In contrast, the S-phase fraction and corresponding radiosensitivity of the population is reduced in marrow samples from ML-prone dogs following hematopoietic recovery. Clearly, these studies have indicated that the cell-cycle properties of the targeted progenitor populations are modified with time of exposure and with pathological progression. However, what is not clear is the extent to which these cell-cycle changes contribute to repair-related functions.

Relative to repair-mediated processes, we know that repair functions are both enhanced and qualitatively modified within radioresistant progenitors, when compared to the radiosensitive progenitors of either unirradiated control animals or AA-prone animals (58,59,63). The following observations support this view: (a) enhanced survival following dose-fractionation (split dose) assays, in vitro; (b) enhanced survival following reduced rates of irradiation, in vitro; (c) ablative action of high-LET neutron irradiation on sublethal damage capacity, i.e., a repair-dependent function; and finally, (d) enhanced capacity to repair single-strand breaks in progenitor DNA as measured by a microfluorometric alkaline elution assay.

Conclusions. In summarizing these studies on the differential hematopathologic responses elicited by chronic ionizing irradiation, there are three points I would like to leave you with. The first is that through combined structural and functional analyses of the hematopoietic tissue responses under continuous, low-daily-dose gamma irradiation, a temporal sequence of pathology-specific preclinical events has been mapped out for the progression of either aplastic anemia or myeloid leukemia. The second is that an early occurring, obligatory leukemogenic phase has been identified and partially characterized; i.e., a phase of hematopoietic recovery that serves to promote, on one hand, the leukemic process, while on the other, restricting progression to aplastic anemia. Finally, the latter hematopoietic recovery event is mediated by a time-dependent selection and amplification of aberrant hematopoietic progenitors that express a battery of newly acquired characteristics, including increased radioresistance, modified cell cycle properties, and enhanced clonal growth and recovery (repair) potentials.

Future Work and Expectations

Unfortunately, I do not have access to a "crystal ball" and, therefore, have serious reservations about speculating how and to what end SEM will be used in future radiobiological investigations. This exercise brings to mind a Mark Twain quote on the wonder of science: "You get such a wholesale return of conjecture for such a trifling investment in fact." Keeping this quote in mind, I will try to make my predictions and suggestions for new areas of study on the conservative side.

Without question, the ultrastructurally oriented radiobiologist will have not only an opportunity to reexamine older problems using newer, more powerful tools, but also will be afforded new and exciting areas to explore. Due to the advent of high resolution EM techniques (5,30,65,71) and the development of a host of new membrane and genetic probes (21,32,33), a number of previously unanswered, fundamentally important, radiobiological questions will no doubt be addressed and subsequently answered. Such questions, for example, concern the physical nature of radiosensitive subcellular targets, e.g., Alper's genomic "N" type-, membranous "O" (2,36,74) type-, and the "N/O" cooperative targets (3,18,19,67,78). Potentially fruitful areas of study, related to genomic targets, might include: (a) the ultrastructural localization and characterization of fragile, radiosensitive sites (i.e., sites of origin of induced breaks, gaps, and translocations) on chromosomes (31,34); and (b) the identification and mapping of various chromosome-specific genes and gene products via in situ DNA/RNA probe

Fig. 29. Reciprocal changes in circulating levels of blood granulocytes and serum levels of GM-CFUa-colony stimulating activity (CSA) relative to the several of the dominant hematopathologies seen under chronic gamma irradiation.

Fig. 30. In vitro radiosensitivity of hematopoietic progenitors (GM-CFUa) from aplasia-prone, leukemia-prone, and unirradiated controls (61).

Figs. 31 and 32. Change in expression of GM-CFUa clonotypes, with varying degrees of radiosensitivity, with time of exposure and preclinical phase. Fig. 31. Progression to aplastic anemia. Fig. 32. Progression to myeloid leukemia (60). Clonotypes: X, normal radiosensitive variety; A, radioresistant, expanded potentially lethal damage (PDL) capacity; B, expanded sublethal damage (SLD) capacity; and C, expanded PDL and SDL capacities.

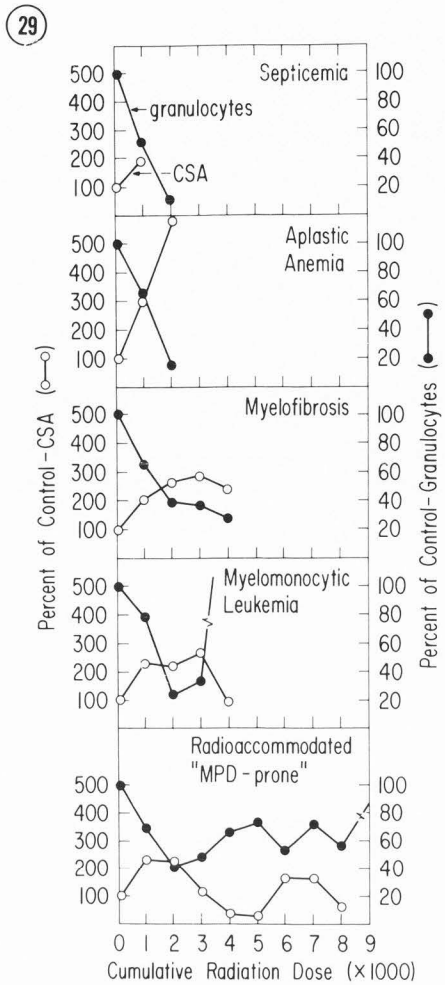

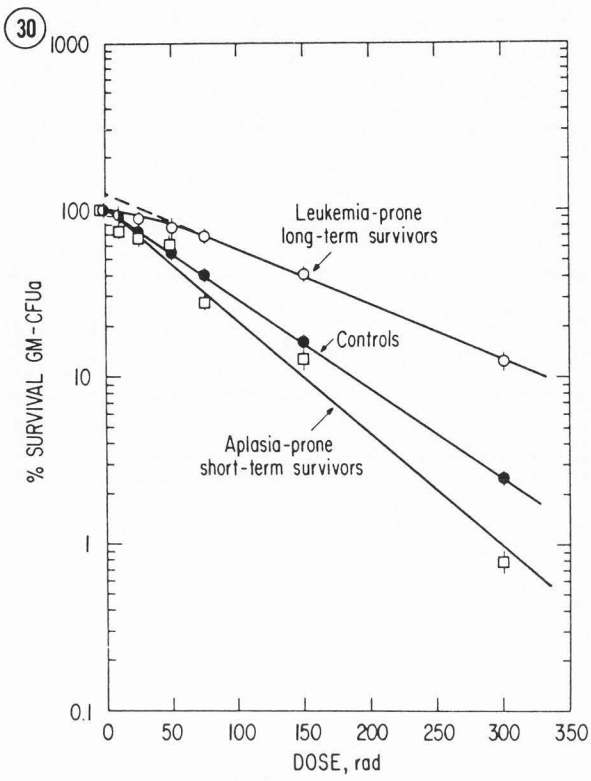

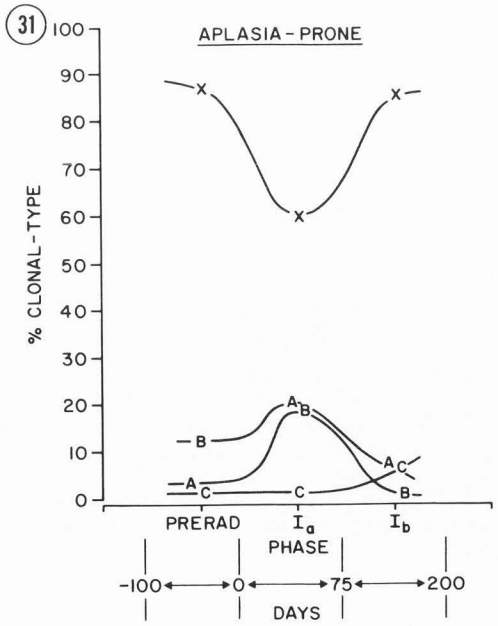

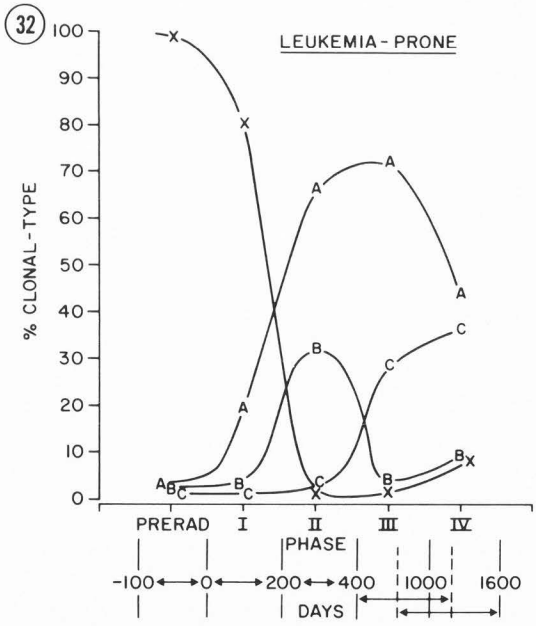

hybridization (33) and high resolution EM (30,31).

Future studies on the nature of vital membrane targets should prove to be equally fruitful. Analogous to the high resolution cytogenetic studies mentioned above, the identification and characterization of key structural elements (transmembrane proteins, transport channels,

etc.) of limiting membranes, as well as distributional mapping, as a function of radiation exposure should provide key insights into both initial and late-arising cellular responses following radiation exposure (36,75,77). In regard to the latter, one of the more important areas in radiobiology today concerns the molecular mechanisms of carcinogenic transformation by ionizing radiation. The process of cell transformation has been clearly demonstrated to be modulated by cell-surface-related events; i.e., radiation-elicited transformation frequencies can be either greatly enhanced or suppressed by pretreating irradiated target cells with surface-active reagents (e.g., enhanced by proteolytic digestion or free radical attack; suppressed by inhibitors of proteolytic enzymes and free radical quenching enzymes) (35). It is reasonable to assume that altered cell surface structures generate signals that are cytoplasmically transduced, received, and processed by the nucleus in terms of the suppression or activation of transforming gene function. Clearly, structural resolution of these vital surface elements via high-resolution EM will serve to define the cooperative interplay of radiosensitive membranous and genomic targets and thus provide insight into basic carcinogenic processes.

Conclusion

Despite the complexities intrinsic to the radiation-induced response, significant advances have been made in defining the nature and the inductive mechanisms. Along with the biochemical, physiological, and metabolic end points used by the radiobiologist in attempting to define early, late, and secondary response patterns, the end point of cell and tissue ultrastructure has been effectively used as well, to provide, in a complementary fashion, direct visual evidence of induced lesions to vital structures.

Therefore, as structure is a vital component of the STRUCTURE + FUNCTION = RESPONSE equation, it becomes critical to continue to examine and explore, with the currently available repertoire of microscopic techniques, structural aspects of the radiation-induced response at the various levels of biological organization.

Acknowledgments

This work was supported by the U. S. Department of Energy, Office of Health and Environmental Research, under contract No. W-31-109-ENG-38. The general support and assistance of TE Fritz, LV Kaspar, DV Tolle, SM Cullen, DE Doyle is gratefully acknowledged, along with the secretarial help of MC D'Arpa.

References

1. Albertsson M, Hakansson CH, von Mecklenburg C. (1983). Scanning electron microscopy and recording of the physiological activity of tracheal ciliated cells treated by fractionated irradiation, Scanning Electron Microsc. 1983; IV: 2019-2026.

2. Alper T. (1971). Cell death and its modification. The role of primary lesions in membranes and DNA, in: Biological Aspects of Radiation Quality, International Atomic Energy Agency, Vienna, 171-184.

3. Alper T. (1979). The target concept and target theory, in: Cellular Radiobiology, Cambridge University Press, Cambridge, 18-32.

4. Anderson JH, Withers RH. (1973). Scanning electron microscope studies of irradiated rat intestinal mucosa, Scanning Electron Microsc. 1973: 566-572.

5. Arro E, Collins VP, Brunk UT. (1981). High resolution SEM of cultured cells: Preparatory procedures, Scanning Electron Microsc. 1981; II: 159-168.

6. Berdjis CC (ed). (1971). Pathology of Irradiation. William & Wilkins Co., Baltimore, MD, 1-31.

7. Borek C, Fenoglio CM. (1976). Scanning electron microscopy of surface features of hamster embryo cells transformed in vitro by X-irradiation, Cancer Res. 36, 1325-1334.

8. Carr KE. (1981). Scanning electron microscopy of tissue response to irradiation, Scanning Electron Microsc. 1981; IV: 35-46.

9. Carr KE, Hamlet R, Nias AHW, Watt C. (1979). Lack of correlation between villus and crypt damage in irradiated mouse intestine, Brit. J. Radiol. 52, 485-493.

10. Carr KE, Hamlet R, Nias AH, Boyle FC, Fife MG. (1985). Stromal damage in the mouse small intestine after Co60 or D-T neutron irradiation, Scanning Electron Microsc. 1985; IV: 1615-1621.

11. Carr KE, Hamlet R, Nias AH, Watt C. (1984). Morphological differences in the response of mouse small intestine to radiobiologically equivalent doses of X and neutron irradiation, Scanning Electron Microsc. 1984; I: 445-454.

12. Carr KE, Hamlet R, Nias AHW, Watt C. (1983). Damage to the surface of the small intestinal villus: An objective scale of assessment of the effects of single and fractionated doses, Brit. J. Radiol. 56, 467-475.

13. Carr KE, Hume SP, Marigold JCL, Michalowski A. (1982). Scanning and transmission electron microscopy of the damage to small intestinal mucosa following X irradiation or hyperthermia, Scanning Electron Microsc. 1982; I: 393-402.

14. Cohen GI, Greenberger JS, Canellos GP. (1982). Effect of chemotherapy and irradiation on interactions between stromal and hemopoietic cells in vitro, Scanning Electron Microsc. 1982; I: 359-365.

15. Committee on the Biological Effects of Ionizing Radiations (BEIR). (1980). Leukemia, in: The Effects on Populations of Exposure to Low Levels of Ionizing Radiation, National Research Council, National Academy Press, Washington, D.C., 398-431.

16. Egawa J, Ishioka K. (1978). Radiation effects on the fine blood vessels in abdominal organs of mice, Acta Radiol. Oncol. 17, 414-422.

17. Elkind MM. (1974). Endpoints and targets in radiobiology, in: Physical Mechanisms in Radiation Biology, Cooper RD, Woods RW (eds), United States Atomic Energy Commission, CONF721001, 296-301.

18. Elkind MM. (1980). Cells, targets, and molecules in radiation biology, in: Radiation Biology in Cancer Research, Meyn RE, Withers HR, (eds), Raven Press, New York, 71-93.

19. Elkind MM, Chang-Liu CM. (1972). Repair of a DNA complex from X-irradiated Chinese hamster cells, Int. J. Radiat. Biol. 22, 75-90.

20. Friberg LG. (1980). Effects of radiation on the small intestine of the rat. A SEM study, Ph.D. thesis, ISBN 91-7222-298-0, Lund University, Sweden.

21. Gilden RV. (1984). Oncogenes, Oncos 1, 1-5.

22. Gong JK. (1978). Endosteal marrow: A rich source of hematopoietic stem cells, Science 199, 1443-1445.

23. Håkansson CH, Von Mecklenburg C. (1981). The effects of ionizing irradiation on the ciliated cells of the central nervous system (CNS) in man--A scanning electron microscopy study, Scanning Electron Microsc. 1981; IV: 93-98.

24. Hamberg H, Brunk UT, Ericsson JLE, Jung B. (1976). Cytoplasmic effects of X-irradiation on cultured cells in a nondividing stage, Acta Path. Microbiol. Scand. A84, 201-214.

25. Hamberg H, Brunk UT, Ericsson JLE, Jung B. (1977). Cytoplasmic effects of X-irradiation on cultured cells in a nondividing stage, Acta Path. Microbiol. Scand. A85, 625-639.

26. Hamberg H, Brunk UT, Ericsson JLE, Jung B. (1978). Cytoplasmic effects of X-irradiation on cultured cells in a nondividing stage, Acta Path. Microbiol. Scand. A86, 487-494.

27. Hamberg H, Brunk UT, Ericsson JLE, Jung B. (1980). Cytoplasmic effects of X-irradiation on cultured cells in a nondividing stage, Acta Path. Microbiol. Scand. A88, 231-239.

28. Hamel HMH, Carr KE, Hume SP, Marigold JCL. (1985). Structural changes in mouse small intestinal villi following lower body hyperthermia, Scanning Electron Microsc. 1985; II: 849-858.

29. Hamlet R, Carr KE, Nias AHW, Watt C. (1981). Surface damage in the small intestine of the mouse after X- or neutron irradiation, Scanning Electron Microsc. 1981; IV: 73-78.

30. Harrison CJ, Allen TD, Britch M, Harris R. (1982). High-resolution scanning electron microscopy of human metaphase chromosomes, J. Cell Sci. 56, 409-422.

31. Harrison CJ, Allen TD, Jack EM, Harris R. (1983). The fragile X, a scanning electron microscope study, J. Med. Gen. 20, 280-285.

32. Horisberger M. (1981). Colloidal gold: A cytochemical marker for light and fluorescent microscopy and for transmission and scanning electron microscopy, Scanning Electron Microsc. 1981; II: 9-32.

33. Hutchison NJ, Langer-Safer RR, Ward DC, Hamkalo BA. (1982). In situ hybridization at the electron microscope level: Hybrid detection by autoradiography and colloidal gold, J. Cell Biol. 95, 609-618.

34. Kano Y, Little JB. (1986). Site-specific chromosomal rearrangements induced in human diploid cells by x-irradiation, Cytogenet. Cell Genet. 41, 22-29.

35. Kennedy AR, Troll W, Little JB. (1984). Role of free radicals in the initiation and promotion of radiation transformation in vitro, Carcinogenesis 5, 1213-1218.

36. Koteles GJ. (1979). New aspects of cell membrane radiobiology and their impact on radiation protection, Atomic Energy Rev. 17, 3-30.

37. Kuo TM, Meinke W, Saunders GF. (1975). Localization of cytoplasmic membrane associated DNA in human chromosomes, Proc. Nat. Acad. Sci. 72, 5004-5006.

38. Lloyd EL, Henning CB. (1981). Morphology of cells malignantly transformed by alpha particle irradiation, Scanning Electron Microsc. 1981; IV: 87-92.

39. Lord BI. (1983). Haemopoietic stem cells, in: Stem Cells, CS Potten (ed), Churchill Livingstone, New York, 118-154.

40. Magee JL, Chatterjee A. (1977). Fundamental radiobiological physics and radiation chemistry of heavy ions in models of chemical and biological effects, in: Biological and Medical Research with Accelerated Heavy Ions at the Bevalac, LBL-5610, University of California, Berkeley, Chapter 5.

41. Maisin JR, Van Gorp U, de Saint-Georges L. (1982). The ultrastructure of the lung after exposure to ionizing radiation as seen by transmission and scanning electron microscopy, Scanning Electron Microsc. 1982; I: 403-412.

42. McLennon G, Oberley LW, Autor AP. (1980). The role of oxygen-derived free radicals in radiation-induced damage and death of non-dividing eucaryotic cells, Radiat. Res. 84, 122-132.

43. Metcalf D. (1977). Hemopoietic Colonies: In Vitro Cloning of Normal and Leukemic Cells, Springer-Verlag, New York, 99-131.

44. Metcalf D. (1983). Regulation of self-replication in normal and leukemic stem cells, in: Normal and Neoplastic Hematopoiesis, DW Golde, PA Marks (eds), Alan R. Liss, Inc., New York, 141-156.

45. Nelson AC, Hayes TL, Tobias CA, Yang TCH. (1981). Some indications of structural damage in retina by heavy ion radiation, Scanning Electron Microsc. 1981; IV: 79-85.

46. Nelson AC, Shah-Yukich A, Babayan R. (1984). Radiation damage in rat kidney microvasculature, Scanning Electron Microsc. 1984; III: 1273-1277.

47. Nelson AC, Wyle HR. (1985). Morphological changes in neutron irradiated red blood cells, Scanning Electron Microsc. 1985; IV: 1623-1630.

48. Newton JC, Barsa-Newton MC, Wardley J. (1980). The effects of X-radiation on the retina of the albino rabbit as viewed with the scanning electron microscope, Radiat. Res. 81, 311-318.

49. Okyama H, Yamada T. (1983). Appearance of cell fragments in thymus after a whole-body x-irradiation of rat, Scanning Electron Microsc. 1983; III: 1339-1343.

50. Patt HM. (1975). Bone marrow regeneration after local injury: A review, Exp. Hematol. 3, 135-146.

51. Penney DP, Siemann DW, Rubin P, Shapiro DL, Finkelstein J, Cooper RA. (1982). Morphologic changes reflecting early and late effects of irradiation of the distal lung of the mouse: A review, Scanning Electron Microsc. 1982; I: 413-425.

52. Philpott DE, Sapp W, Kato K, Corbett R, Stevenson J, Black S, Lindseth KA, Benton EV. (1985). The effect of high energy (HZE) particle radiation (40Ar) on aging parameters of mouse hippocampus and retina, Scanning Electron Microsc. 1985; III: 1177-1182.

53. Porvaznik M. (1979). Tight junction disruption and recovery after sublethal X-irradiation, Radiat. Res. 78, 233-250.

54. Seed TM, Carr KE. (1983). Ultrastructural effects of radiation on tissues and cells: Concluding remarks, in: Ultrastructural Effects of Radiation on Tissues and Cells, Carr KE, Seed TM (eds), 167-168, Scanning Electron Microscopy, Inc., AMF O'Hare, Chicago, Illinois.

55. Seed TM, Chubb GT, Tolle DV. (1981). Sequential changes in bone marrow architecture during continuous low dose gamma irradiation, Scanning Electron Microsc. 1981; IV: 61-72.

56. Seed TM, Chubb GT, Tolle DV, Fritz TE, Poole CM, Doyle DE, Lombard LS, Kaspar LV. (1982). The ultrastructure of radiation-induced endosteal myelofibrosis in the dog, Scanning Electron Microsc. 1982; I: 377-391.

57. Seed TM, Chubb GT, Ulrich RG, Wright BJ, Kaspar LV. (1979). Preparation and observation by SEM of hemopoietic cells cloned in soft agar, Scanning Electron Microsc. 1979; III: 397-410.

58. Seed TM, Kaspar LV. (1986). Radiosensitivity of hemopoietic progenitors during preclinical phases of progressing radiation-induced myeloproliferative disease. 34th Annual Meeting, Radiation Research Society, Las Vegas, NV, April 12-17, 1986, #DN-9 (available from author).

59. Seed, TM, Kaspar LV, Grdina DJ. (1986). Hematopoietic repair modifications during preclinical phases of chronic radiation-induced myeloproliferative disease, Exp. Hematol. 14, 443.

60. Seed TM, Kaspar LV, Fritz TE, Tolle DV. (1985). Cellular responses in chronic radiation leukemogenesis, in: Carcinogenesis, E Huberman, SH Barr (eds), Raven Press, New York, 363-379.

61. Seed TM, Kaspar LV, Tolle CV, Fritz TE. (1982). Hematologic predisposition and survival time under continuous gamma irradiation: Responses mediated by altered radiosensitivity of hemopoietic progenitors, Exp. Hematol. 10(12), 232-248.

62. Seed TM, Kaspar LV, Tolle DV, Poole CM, Fritz TE. (1981). Clonal growth patterns of granulocyte progenitors from beagle dogs with myeloid leukemia, Exp. Hematol. 9(9), 68.

63. Seed TM, Kaspar LV, Tolle DV, Fritz TE. (1983). Acquired radioresistance of hematopoietic progenitors under continuous low daily dose gamma irradiation, Exp. Hematol. 11(14), 137.

64. Seed TM, Tolle DV, Fritz TE, Cullen SM, Kaspar LV, Poole CM. (1978). Haemopathological consequences of protracted gamma irradiation in the beagle: Preclinical phases of leukemia induction, in: Late Biological Effects of Ionizing Radiation, IAEA-SM-224/308, International Atomic Energy Agency, Vienna, 531-549.

65. Soligo D, Lampen N, de Harven E. (1981). Backscatter electron imaging of human leukocytes, Scanning Electron Microsc. 1981; II: 95-104.

66. Somosy Z, Kubasova T, Koteles GT. (1983). Scanning electron microscopic appearance of X-irradiated human fibroblasts, J. Radiat. Res. 24, 109-117.

67. Strazhevskaya NB, Struchkov VA. (1977). Organization of supramolecular DNA complexes of eukaryotic chromatin and their role in the radiation effect, Radiobiologiya 17, 163-177.

68. Szekely JG, Copps TP. (1976). Radiation-induced delay of nuclear pore formation, J. Cell Biol. 70, 466-470.

69. Szekely JG, Raaphorst GP, Lobreau AU, Copps TP. (1982). Effect of X-irradiation and radiation modifiers on cellular ultrastructure, Scanning Electron Microsc. 1982; I: 335-347.

70. Szekely JG, Raaphorst GP, Lobreau AU, Azzam EI, Vadasz JA. (1985). Growth of a radiation-transformed clone of C3H 10T1/2 cells into melanin-producing colonies, Scanning Electron Microsc. 1985; IV: 1631-1640.

71. Tanaka K. (1981). Demonstration of intracellular structures by high resolution scanning electron microscopy, Scanning Electron Microsc. 1981; II: 1-8.

72. Tavassoli M. (1982). Ultrastructural and radiobiological characterization of stromal cells in continuous long-term marrow culture, Scanning Electron Microsc. 1982; I: 349-357.

73. Tolle DV, Seed TM, Cullen SM, Poole CM, Fritz TE. (1982). Aberrant megakaryocytopoiesis preceding radiation-induced leukemia in the dog, Scanning Electron Microsc. 1982; I: 367-376.

74. Walker RI, Brook I, Costerton JW, MacVittie T, Mykal ML. (1985). Possible association of mucous blanket integrity with postirradiation colonization resistance, Radiat. Res. 104, 346-357.

75. Wallach DFH. (1974). Radiation effects on biomembranes, in: Biomembranes, Manson LA (ed), Plenum Press, New York, 213-249.

76. Yamada T, Ohyama H. (1981). Disappearance of microvilli accompanying radiation-induced interphase death of rat thymocytes, Scanning Electron Microsc. 1981; IV: 55-60.

77. Yau TM. (1981). Alterations in the structure and function of the mammalian cell membrane after exposure to ionizing radiation, Scanning Electron Microsc. 1981; IV: 47-54.

78. Zermeno A, Cole A. (1969). Radiosensitive structure of metaphase and interphase hamster cells as studied by low voltage electron beam irradiation, Radiat. Res. 39, 669-684.

Discussion with Reviewers

J. G. Szekely: Could you describe briefly what happens in "fraction-of-life" irradiations? If the irradiation is stopped during the preclinical phase, for example, do the S^- and R^+ subgroups repair and return to the initial state, or do they continue to develop into AA- or ML-prone animals?
Author: The earlier the radiation exposure is terminated, the lower the probability the S^- and R^+ animals will progress to either aplastic anemia (AA) or myeloid leukemia (ML), respectively. Relative to R^+ individuals, if the irradiation is stopped prior to hematopoietic recovery (i.e., ~200 days of exposure at 7.5 rad/day), the risk of developing ML drops off (approaches 0%, as indicated by tentative results obtained to date; Seed et al., Leukemia Res. In press). However, these animals do not become free of pathologic risk, i.e., they are not repaired in an error-free manner; the frequency of solid-type tumors increased significantly, especially in those animals receiving large accumulated radiation doses.

J. G. Szekely: You mentioned that AA-prone dogs had lower SDD levels than controls. This can't explain the radiation resistance of ML-prone subgroups, but can it account for the increased AA-prone cell sensitivity?
Author: Perhaps. Additional experiments are needed, however, to explore and to verify this assumption.

J. G. Szekely: Have any of the hematopoietic tissue been extended to other breeds of dogs or other animals?
Author: No, not to my knowledge.

M. Tavassoli: What is the proportion of AA-prone and ML-prone individuals in any defined group of dogs? Does this proportion change from one group to the other? Is it possible that a genetic predisposition may play a role here?
Author: Under continuous duration-of-life exposures at 7.5 rad/day, the proportion of S^- and R^+ dogs is ~60/40 for all dogs tested to date. Within a limited range, the proportion of S^- and R^+ dogs within smaller selected groups does appear to change, e.g., from 50/50 to 80/20, etc. It is likely that the pathologic predispositions expressed by these subgroups are genetically based. Based on preliminary cytogenetic work, we have identified a characteristic 1st chromosome translocation within the R^+ individuals following prolonged periods of irradiation. How early in the course of exposure this chromosomal change occurs remains to be determined.

M. Tavassoli: In view of the recent evidence that indicates the membrane receptor for CSA is a gene product of fms oncogene, the fall in CSA levels in MPD-prone groups (documented in Figure 29) raises the question that the expression of such a gene may increase the numbers of receptors for CSA, leading to its binding and, hence, a fall in the serum CSA.
Author: This is an interesting possibility. I've always considered the rise and fall of serum CSA to reflect the change in number of targeted progenitors in the marrow. With renewed progenitor cell proliferation, CSA levels might be expected to fall due to the negative "feedback," but perhaps an even faster decline would be expected if those self-renewing progenitors had increased numbers of CSA surface-binding receptors.

T. D. Allen: Do the adipocytes increase in number as a primary event--displacing the free haematopoietic cells--, or as a "space-filling" response to the decline of haemopoietic cells?
Author: This question has been asked by hematologists many times before and, to my knowledge, has not yet been answered satisfactorily. The "space-filling" concept is more commonly accepted, however we see situations where there is, simultaneously, both low cellularity and low-fat content in the marrow (e.g., in the regenerating hematopoietic phase, described here for evolving

ML). Although supporting experimental evidence is lacking, it is my own feeling that neither situation (i.e., increased adipocytes as a primary event, or increased adipocytes as space-fillers) is correct, but rather that the extent of the free hematopoietic cell-stroma interactions dictates the extents of adipogenesis in much the same way as it does overall hematopoietic progenitor cell proliferation.

T. D. Allen: Does the difference between the leukaemia and aplastic anaemia indicate, perhaps, the presence of a complementary stimulation between stroma and haematopoietic cells which is blocked in aplastic anaemia leading to the aplasia, but not in the leukaemia?
Author: This is a real possibility--one that probably should be explored experimentally in vitro. Some time ago, we started to evaluate, by co-cultivation, the regulatory and feeding capacity of stroma from aplastic anemia-prone and leukemia-prone dogs in terms of maintenance and proliferative capacity of lineage-committed hematopoietic progenitors derived not only from unirradiated controls but also from aplasia-prone and leukemia-prone irradiated dogs. Although these studies were fraught with technical problems, we did observe less "feeding capacity" with stroma from the aplasia-prone dogs.

Additional Reference

Seed TM, Kaspar LV, Tolle DV, Fritz TE. Chronic radiation leukemogenesis: Postnatal hematopathologic effects resulting from in utero irradiation. Leukemia Res., in press.